

# Local Thermal Non-equilibrium and Heterogeneity Effects on the Onset of Double-Diffusive Convection in an Internally Heated and Solute-d Porous Medium

A. V. Kuznetsov<sup>1</sup> · D. A. Nield<sup>2</sup> · A. Barletta<sup>3</sup> · M. Celli<sup>3</sup>

Received: 27 March 2015 / Accepted: 29 May 2015 / Published online: 12 June 2015  
© Springer Science+Business Media Dordrecht 2015

**Abstract** The effect of local thermal non-equilibrium on the onset of double-diffusive convection in a porous medium consisting of two horizontal layers, each internally heated, is studied analytically. Linear stability theory is applied. Variations of permeability, fluid thermal conductivity, solid thermal conductivity, heat source strength in the solid and fluid phases, concentration source strength, interphase heat transfer coefficient and porosity are considered. In addition to the major effects from heterogeneity of permeability, fluid thermal conductivity and heat source strength in the fluid phase as with single-diffusive convection, it is now found that major effects arise from heterogeneity of solutal source strength and porosity. We used two different methods to obtain our results. Analytical results that readily show the effects of parameter variations were obtained by using a low-term Galerkin approximation, which was validated by using a highly accurate numerical solver. Since for a problem with large number of parameters simple analytical results are highly desirable, the quantification of the accuracy of a low-term Galerkin approximation presented in our paper is quite important.

---

✉ A. V. Kuznetsov  
avkuznet@ncsu.edu

D. A. Nield  
d.nield@auckland.ac.nz

A. Barletta  
antonio.barletta@unibo.it

M. Celli  
michele.celli3@unibo.it

<sup>1</sup> Department of Mechanical and Aerospace Engineering, North Carolina State University, Campus Box 7910, Raleigh, NC 27695-7910, USA

<sup>2</sup> Department of Engineering Science, University of Auckland, Private Bag 92019, Auckland 1142, New Zealand

<sup>3</sup> Department of Industrial Engineering, Alma Mater Studiorum Università di Bologna, Viale Risorgimento, 2, 40136 Bologna, Italy

**Keywords** Local thermal non-equilibrium · Porous medium · Instability · Natural convection · Heterogeneity · Double diffusion

## List of symbols

$a$	Dimensionless horizontal wavenumber
$C$	Dimensionless concentration, $\frac{(\rho c)_f \rho_0 g \beta_C K_1 H}{\mu k_{f1}} (C^* - C_0)$
$C^*$	Solute concentration
$C_0$	Solute concentration at each of the upper and lower boundaries
$D$	$d/dz$
$D_C$	Solutal diffusivity
$h$	Interface heat transfer coefficient (incorporating the specific surface area) between the fluid and solid particles
$\hat{h}$	Parameter defined in Eq. (18)
$h_r$	Interface heat transfer coefficient ratio, $h_2/h_1$
$g$	Gravitational acceleration
$\mathbf{g}$	Gravitational acceleration vector
$H$	Dimensional layer depth
$k$	Thermal conductivity
$k_f$	Thermal conductivity of the fluid phase
$\hat{k}_f$	Parameter defined in Eq. (18)
$k_{f1}$	Fluid thermal conductivity ratio, $k_{f2}/k_{f1}$
$k_s$	Thermal conductivity of the solid phase
$\hat{k}_s$	Parameter defined in Eq. (18)
$k_{s1}$	Solid thermal conductivity ratio, $k_{s2}/k_{s1}$
$K$	Permeability of the porous medium
$K_r$	Permeability ratio, $K_2/K_1$
$\hat{K}$	Parameter defined in Eq. (18)
$Le$	Lewis number, $\frac{k_{f1}}{(\rho c)_f D_C}$
$N$	Interface heat transfer parameter, $\frac{h_1 H^2}{\phi_1 k_{f1}}$
$P$	Dimensionless pressure, $\frac{(\rho c)_f K_1}{\mu k_{f1}} P^*$
$P^*$	Pressure, excess over hydrostatic
$Q$	Volumetric heat source strength
$Q_C$	Volumetric solute source strength
$\hat{Q}_C$	Parameter defined in Eq. (18)
$Q_{Cr}$	Solute source ratio, $Q_{C2}/Q_{C1}$
$\hat{Q}_f$	Parameter defined in Eq. (18)
$Q_{fr}$	Heat source ratio in the fluid phase, $Q_{f2}/Q_{f1}$
$\hat{Q}_s$	Parameter defined in Eq. (18)
$Q_{sr}$	Heat source ratio in the solid phase, $Q_{s2}/Q_{s1}$
$Ra$	Internal thermal Rayleigh number, $\frac{(\rho c)_f \rho_0 g \beta_C K_1 H^3 Q_{f1}}{2\mu k_{f1}^2}$
$Ra_C$	Internal solutal Rayleigh number, $\frac{(\rho c)_f \rho_0 g \beta_C K_1 H^3 Q_{C1}}{2\mu k_{f1}^2 D_C}$
$Ra_{\text{eff}}$	Effective combined Rayleigh number defined in Eq. (63)
$t$	Dimensionless time, $\frac{k_{f1}}{(\rho c)_f H^2} t^*$
$t^*$	Time
$T$	Dimensionless temperature, $\frac{(\rho c)_f \rho_0 g \beta_C K_1 H}{\mu k_{f1}} (T^* - T_0)$

$T^*$	Temperature
$T_0$	Temperature at each of the upper and lower boundaries
$(u, v, w)$	Dimensionless velocity components, $\frac{(\rho c)_f H}{k_{f1}} (u^*, v^*, w^*)$
$\mathbf{u}^*$	Darcy velocity, $(u^*, v^*, w^*)$
$(x, y, z)$	Dimensionless Cartesian coordinates, $(x^*, y^*, z^*)/H$ ; $z$ is the vertically upward coordinate
$(x^*, y^*, z^*)$	Cartesian coordinates; $z^*$ is the vertically upward coordinate

### Greek symbols

$\alpha$	Modified thermal diffusivity ratio, $\frac{(\rho c)_{s1} k_{f1}}{(\rho c)_f k_{s1}}$
$\beta$	Thermal expansion coefficient of the fluid
$\beta_C$	Solutal expansion coefficient of the fluid
$\gamma$	Modified thermal conductivity ratio, $\frac{\phi_1 k_{f1}}{(1-\phi_1)k_{s1}}$
$\delta$	Dimensionless layer depth ratio (interface position)
$\hat{\delta}$	Parameter defined in Eq. (18)
$\delta_r$	Inverse solid fraction ratio, $\frac{1-\phi_1}{1-\phi_2}$
$\hat{\varepsilon}$	Parameter defined in Eq. (18)
$\varepsilon_r$	Solid heat capacity ratio, $\frac{(\rho c)_{s2}}{(\rho c)_{s1}}$
$\mu$	Viscosity of the fluid
$\rho_0$	Fluid density at temperature $T_0$
$\rho_f$	Fluid density
$(\rho c)_f$	Heat capacity of the fluid
$(\rho c)_s$	Heat capacity of the solid
$\phi$	Porosity
$\hat{\phi}$	Parameter defined in Eq. (18)
$\phi_r$	Porosity ratio, $\phi_2/\phi_1$

### Subscripts

B	Basic state
f	Fluid phase
r	Relative quantity
s	Solid phase
1	The region $0 \leq z^* < \delta H$
2	The region $\delta H \leq z^* \leq H$

### Superscripts

'	Perturbation variable
*	Dimensional variable

## 1 Introduction

Recently the present authors have been sorting out the important interactions between the effects of various agencies that remove the symmetry (about the mid-plane) in the onset of convection in a horizontal layer occupied by a porous medium with symmetric boundary conditions. These agencies include vertical heterogeneity and vertical throughflow. The situation

is complicated when there is local thermal non-equilibrium (LTNE, see [Patil and Rees 2013](#)) because then heterogeneity of the interphase heat transfer is involved, throughflow occurs only in the fluid phase, and the heterogeneity of each of fluid conductivity and solid conductivity are pertinent. A further complication occurs in the double-diffusive situation because convection of a solute can occur only in the fluid phase. The effects of heterogeneity (with a layered medium) and LTNE diffusion (but not throughflow) were studied by [Nield and Kuznetsov \(2013\)](#) for the double-diffusive case. In each case, the medium was heated from below.

In the present paper, the study in [Nield and Kuznetsov \(2014\)](#) is repeated, but now for the case of internal heating rather than bottom heating. With internal heating, the basic vertical temperature gradient changes sign, from positive in the lower part of the domain to negative in the upper part, and as a result most of the convection, when it occurs, takes place in the upper part. Thus vertical heterogeneity now plays a greater role. The present paper is an extension, to the case of double diffusion, of the work by [Kuznetsov and Nield \(2014\)](#). Besides having a uniform volumetric heat source, we now have a uniform volumetric solute source. As far as we are aware, this combination has not been studied previously, even in the case of a homogeneous medium with LTE. A new internal solutal Rayleigh number is introduced.

Possible applications include a situation where the fluid and/or the solid is radioactive, and one in which there is solute deposition.

The authors have written a companion paper for the case of bottom heating ([Nield et al. 2015](#)). For completeness we cite two more of our papers on closely connected topics. In these only single diffusion is involved and bottom heating rather than internal heating is discussed, but other extensions are made. In [Kuznetsov and Nield \(2015\)](#) and [Nield and Kuznetsov \(2014\)](#), the effect of vertical throughflow is included. In the latter, the effect of heterogeneity is added to the mix.

The following analysis is closely similar to that in our previous papers, and so, the presentation has been shortened where that is possible.

## 2 Analysis

### 2.1 General Equations

Asterisks are used to denote dimensional variables. The  $z^*$ -axis is taken in the upward vertical direction, and the porous medium is unbounded in the  $x^*$  and  $y^*$  directions. Subscripts 1 and 2 are used to denote the two layers, of depths  $\delta H$  and  $(1 - \delta)H$ , where  $\delta$  is less than unity. The first occupies the region  $0 \leq z^* < \delta H$ , and the second occupies the region  $\delta H \leq z^* \leq H$ . A uniform temperature  $T_0$  and a uniform concentration  $C_0$  are imposed at each of the upper and lower boundaries.

The Oberbeck–Boussinesq approximation is invoked. The equations representing the conservation of mass, Darcy’s law, and the conservation of thermal energy for each phase, and the conservation of solute, take the form

$$\nabla^* \cdot \mathbf{u}^* = 0, \tag{1}$$

$$0 = -\nabla^* P^* - \frac{\mu}{K} \mathbf{u}^* - \rho_0 [\beta(T_f^* - T_0) + \beta_C(C_f^* - C_0)] \mathbf{g}, \tag{2}$$

$$\phi(\rho c)_f \left[ \frac{\partial T_f^*}{\partial t^*} + \mathbf{u}^* \cdot \nabla^* T_f^* \right] = \phi k_f \nabla^{*2} T_f^* + h(T_s^* - T_f^*) + \phi Q_f, \tag{3}$$

$$(1 - \phi)(\rho c)_s \frac{\partial T_s^*}{\partial t^*} = (1 - \phi)k_s \nabla^{*2} T_s^* + h(T_f^* - T_s^*) + (1 - \phi)Q_s, \tag{4}$$

$$\phi \frac{\partial C^*}{\partial t^*} + \mathbf{u}^* \cdot \nabla^* C^* = \phi D_C \nabla^{*2} C^* + \phi Q_C, \tag{5}$$

where

$$\begin{aligned} \phi &= \phi_1, K = K_1, k_f = k_{f1}, k_s = k_{s1}, h = h_1, \\ Q_f &= Q_{f1}, Q_s = Q_{s1}, Q_C = Q_{C1} \text{ in } 0 \leq z^* < \delta H, \\ \phi &= \phi_2, K = K_2, k_f = k_{f2}, k_s = k_{s2}, h = h_2, \\ Q_f &= Q_{f2}, Q_s = Q_{s2}, Q_C = Q_{C2} \text{ in } \delta H < z^* \leq H. \end{aligned} \tag{6}$$

Here the Darcy velocity is denoted by  $\mathbf{u}^* = (u^*, v^*, w^*)$ , where  $t^*$  is the time,  $P^*$  is the pressure (excess over hydrostatic),  $T^*$  is the temperature and  $C^*$  is the solute concentration, while  $K$  is the permeability,  $\phi$  is the porosity,  $k_f$  and  $k_s$  are the thermal conductivities in the fluid and solid phases, respectively,  $(\rho c)_f$  and  $(\rho c)_s$  are the heat capacities of the fluid and the solid, respectively,  $D_C$  is the diffusivity of the solute,  $\mu$  is the fluid viscosity,  $\rho_0$  is the fluid density at temperature  $T_0$ ,  $\beta$  is the thermal expansion coefficient of the fluid,  $\beta_C$  is the corresponding solutal coefficient, and  $\mathbf{g}$  is the gravitational acceleration vector. The standard formulation of Darcy’s law, in which time derivatives are assumed to be negligible, has been adopted in Eq. (2). Since we consider a situation in which the thermal conductivity in each phase is piecewise constant, spatial derivatives of  $k_f$  and  $k_s$  do not appear in Eqs. (3) and (4), where the interface heat transfer coefficient (incorporating the specific surface area) between the fluid and solid particles is denoted by  $h$ . The flow is assumed to be slow so that an advective term and a Forchheimer quadratic drag term do not appear in the momentum equation. It has been assumed that there are uniform volumetric heat sources (with averages taken over representative elementary volumes)  $Q_1$  and  $Q_2$  in the respective layers, and uniform volumetric solute sources (resulting, for example, from the process of dissolution) of  $Q_{C1}$  and  $Q_{C2}$  (assumed to be in the fluid phase in the subsequent analysis) in the respective layers.

We suppose that the upper and lower boundaries are both impermeable. At the interface between the two regions, the normal velocity and the pressure are continuous. Thus the hydrodynamic boundary conditions are

$$w_1^* = 0 \text{ at } z^* = 0, w_2^* = 0 \text{ at } z^* = H, \tag{7a,b}$$

$$w_1^* = w_2^* \text{ and } \frac{1}{K_1} \frac{\partial w_1^*}{\partial z^*} = \frac{1}{K_2} \frac{\partial w_2^*}{\partial z^*} \text{ at } z^* = \delta H. \tag{8a,b}$$

Equation (8b) expresses the continuity of pressure at the interface, and the momentum equation has been used to get this form.

We also suppose that the upper and lower boundaries are both perfectly conducting, and hence, one has local thermal equilibrium there, and also that the concentration is held constant there. At the interface between the two regions, we assume that the temperature and heat flux in each phase are continuous (see [Nield 2012](#)), and likewise the concentration and solute flux are continuous. Thus for the thermal boundary conditions we take

$$T_f^* = T_s^* = T_0, C^* = C_0 \text{ at } z^* = 0 \text{ and at } z^* = H, \tag{9a,b,c,d,e,f}$$

$$T_{f1}^* = T_{f2}^*, T_{s1}^* = T_{s2}^*, C_1^* = C_2^*,$$

$$k_{f1} \frac{\partial T_{f1}^*}{\partial z} = k_{f2} \frac{\partial T_{f2}^*}{\partial z^*}, k_{s1} \frac{\partial T_{s1}^*}{\partial z^*} = k_{s2} \frac{\partial T_{s2}^*}{\partial z^*}, \phi_1 \frac{\partial C_1^*}{\partial z^*} = \phi_2 \frac{\partial C_2^*}{\partial z^*} \text{ at } z^* = \delta H.$$

$$\tag{10a,b,c,d,e,f}$$

The heat flux solid–fluid interface conditions given by Eq. (10d,e) are not the only ones that one could impose. Two conditions need to be specified, and the heat flux could be divided between the two phases in various ways. Alternatives are discussed by Nield (2012). In the absence of any further information, we believe that the choice which makes the best physical sense is the one made here.

We introduce dimensionless variables as follows. For simplicity, we chose to scale in terms of quantities pertaining to region 1. If any adjustments for weighted algebraic mean quantities are desirable, then these can be made later.

We define

$$\begin{aligned}
 (x, y, z) &= \frac{1}{H}(x^*, y^*, z^*), t = \frac{k_{f1}}{(\rho c)_f H^2} t^*, \\
 (u, v, w) &= \frac{(\rho c)_f H}{k_{f1}}(u^*, v^*, w^*), P = \frac{(\rho c)_f K_1}{\mu k_{f1}} P^*, \\
 T_{f1} &= \frac{(\rho c)_f \rho_0 g \beta K_1 H}{\mu k_{f1}}(T_{f1}^* - T_0), T_{s1} = \frac{(\rho c)_f \rho_0 g \beta K_1 H}{\mu k_{f1}}(T_{s1}^* - T_0), \\
 T_{f2} &= \frac{(\rho c)_f \rho_0 g \beta K_1 H}{\mu k_{f1}}(T_{f2}^* - T_0), T_{s2} = \frac{(\rho c)_f \rho_0 g \beta K_1 H}{\mu k_{f1}}(T_{s2}^* - T_0), \\
 C_1 &= \frac{(\rho c)_f \rho_0 g \beta_C K_1 H}{\mu k_{f1}}(C_1^* - C_0), C_2 = \frac{(\rho c)_f \rho_0 g \beta_C K_1 H}{\mu k_{f1}}(C_2^* - C_0).
 \end{aligned}
 \tag{11}$$

$$\tag{12}$$

Equations (1–5), now written explicitly for the case of two regions, take the form:

$$\nabla \cdot \mathbf{u} = 0, \tag{13}$$

$$0 = -\nabla p - \frac{1}{\hat{K}} \mathbf{u} + (T_f + C) \hat{\mathbf{e}}_z, \tag{14}$$

$$\frac{\partial T_f}{\partial t} + \mathbf{u} \cdot \nabla T_f = \hat{k}_f \nabla^2 T_f + \frac{\hat{h}}{\hat{\phi}} N(T_s - T_f) + 2 \hat{Q}_f Ra, \tag{15}$$

$$\hat{\varepsilon} \alpha \frac{\partial T_s}{\partial t} = \hat{k}_s \nabla^2 T_s + \hat{\delta} \hat{h} \gamma N(T_f - T_s) + 2 \hat{Q}_s Ra, \tag{16}$$

$$Le \frac{\partial C}{\partial t} + \frac{Le}{\hat{\phi}} \mathbf{u} \cdot \nabla C = \nabla^2 C + 2 \hat{Q}_C Ra_C, \tag{17}$$

where, for  $0 \leq z < \delta$ ,

$$\hat{K} = 1, \hat{k}_f = 1, \hat{k}_s = 1, \hat{\phi} = 1, \hat{h} = 1, \hat{\delta} = 1, \hat{\varepsilon} = 1, \hat{Q}_f = 1, \hat{Q}_s = 1, \hat{Q}_C = 1, \tag{18a}$$

and, for  $\delta < z \leq 1$ ,

$$\begin{aligned}
 \hat{K} &= K_r, \hat{k}_f = k_{fr}, \hat{k}_s = k_{sr}, \hat{\phi} = \phi_r, \hat{h} = h_r, \\
 \hat{\delta} &= \delta_r, \hat{\varepsilon} = \varepsilon_r, \hat{Q}_f = Q_{fr}, \hat{Q}_s = Q_{sr}, \hat{Q}_C = Q_{Cr},
 \end{aligned}
 \tag{18b}$$

where

$$\begin{aligned}
 K_r &= \frac{K_2}{K_1}, k_{fr} = \frac{k_{f2}}{k_{f1}}, k_{sr} = \frac{k_{s2}}{k_{s1}}, \phi_r = \frac{\phi_2}{\phi_1}, h_r = \frac{h_2}{h_1}, \\
 \delta_r &= \frac{1 - \phi_1}{1 - \phi_2}, \varepsilon_r = \frac{(\rho c)_{s2}}{(\rho c)_{s1}}, Q_{fr} = \frac{Q_{f2}}{Q_{f1}}, Q_{sr} = \frac{Q_{s2}}{Q_{s1}}, Q_{Cr} = \frac{Q_{C2}}{Q_{C1}}.
 \end{aligned}
 \tag{19}$$

We have also defined

$$Ra = \frac{(\rho c)_f \rho_0 g \beta K_1 H^3 Q_{f1}}{2 \mu k_{f1}^2}, Ra_C = \frac{(\rho c)_f \rho_0 g \beta_C K_1 H^3 Q_{C1}}{2 \mu k_{f1} D_C}, \tag{20a,b}$$

$$\alpha = \frac{(\rho c)_{s1} k_{f1}}{(\rho c)_{f1} k_{s1}}, N = \frac{h_1 H^2}{\phi_1 k_{f1}}, \gamma = \frac{\phi_1 k_{f1}}{(1 - \phi_1) k_{s1}}, Le = \frac{k_{f1}}{(\rho c)_f DC}. \tag{21a,b,c,d}$$

Here  $N$  is an interface heat transfer parameter. [Vadász \(2006\)](#) called this type of parameter the Nield number, citing [Nield \(1998\)](#). The parameters  $\alpha$  and  $\gamma$  are modified thermal diffusivity and thermal conductivity ratios, respectively, and  $Le$  is a Lewis number.

The boundary and matching conditions become

$$w_1 = 0, T_{f1} = 0, T_{s1} = 0, C_1 = 0 \text{ at } z = 0, \tag{22a,b,c}$$

$$w_2 = 0, T_{f2} = 0, T_{s2} = 0, C_2 = 0 \text{ at } z = 1, \tag{23a,b,c}$$

$$W_1 = W_2, \frac{\partial W_1}{\partial z} = \frac{1}{K_r} \frac{\partial W_2}{\partial z}, T_{f1} = T_{f2}, T_{s1} = T_{s2}, C_1 = C_2, \\ \frac{\partial T_{f1}}{\partial z} = k_{fr} \frac{\partial T_{f2}}{\partial z}, \frac{\partial T_{s1}}{\partial z} = k_{sr} \frac{\partial T_{s2}}{\partial z}, \frac{\partial C_1}{\partial z} = \phi_r \frac{\partial C_2}{\partial z} \text{ at } z = \delta. \tag{24a,b,c,d,e,f,g,h}$$

### 2.2 Basic Solution

We seek a time-independent quiescent solution of Eqs. (13–17) with temperatures and concentration varying in the  $z$ -direction only, that is a solution of the form

$$\mathbf{u} = 0, P = P_B(z), T_f = T_{fB}(z), T_s = T_{sB}(z), C = C_B(z), \tag{25}$$

subject to the boundary and initial conditions (22–24). Equations (14–17) reduce to

$$0 = -\frac{dP_B}{dz} + T_{fB} + C_B, \tag{26}$$

$$\hat{k}_f \frac{d^2 T_{fB}}{dz^2} + \frac{\hat{h}}{\hat{\phi}} N(T_{sB} - T_{fB}) + 2\hat{Q}_f Ra = 0, \tag{27}$$

$$\hat{k}_s \frac{d^2 T_{sB}}{dz^2} + \delta \hat{h} \gamma N(T_{fB} - T_{sB}) + 2\hat{Q}_s Ra = 0, \tag{28}$$

$$\frac{d^2 C}{dz^2} + 2\hat{Q}_C Ra_C = 0. \tag{29}$$

We now write these equations explicitly for the two regions.

Equations (27–29) in explicit form are

$$\frac{d^2 T_{fB1}}{dz^2} + N(T_{sB1} - T_{fB1}) + 2Ra = 0, \tag{30a}$$

$$\frac{d^2 T_{sB1}}{dz^2} + \gamma N(T_{fB1} - T_{sB1}) + 2Ra = 0, \tag{30b}$$

$$\frac{d^2 C_1}{dz^2} + 2Ra_C = 0, \tag{30c}$$

$$k_{fr} \frac{d^2 T_{fB2}}{dz^2} + \frac{h_r}{\phi_r} N(T_{sB2} - T_{fB2}) + 2Q_{fr} Ra = 0, \tag{30d}$$

$$k_{sr} \frac{d^2 T_{sB2}}{dz^2} + \delta_r h_r \gamma N(T_{fB2} - T_{sB2}) + 2Q_{sr} Ra = 0, \tag{30e}$$

$$\frac{d^2 C_2}{dz^2} + 2Q_{Cr} Ra_C = 0. \tag{30f}$$

These equations must be solved subject to the boundary and interface conditions

$$T_{fB1}(0) = 0, T_{sB1}(0) = 0, C_{B1}(0) = 0, \tag{31a,b,c}$$

$$T_{fB2}(1) = 0, T_{sB2}(1) = 0, C_{B2}(1) = 0, \tag{31d,e,f}$$

$$T_{fB1}(\delta) = T_{fB2}(\delta), T_{sB1}(\delta) = T_{sB2}(\delta), C_{B1}(\delta) = C_{B2}(\delta), \tag{31g,h,i}$$

$$\frac{dT_{fB1}}{dz}(\delta) = k_{fr} \frac{dT_{fB2}}{dz}(\delta), \frac{dT_{sB1}}{dz}(\delta) = k_{sr} \frac{dT_{sB2}}{dz}(\delta), \frac{dC_{B1}}{dz}(\delta) = \phi_r \frac{dC_{B2}}{dz}(\delta). \tag{31j,k,l}$$

The solutal equations are decoupled from the thermal equations and have the solution

$$C_{B1} = Ra_C \left\{ \left[ \frac{\phi_r Q_{Cr} [1 + (2\phi_r - 1)\delta^2] - \phi_r \delta^2}{1 + (\phi_r - 1)\delta} + 2\delta(1 - \phi_r Q_{Cr}) \right] z - z^2 \right\}, \tag{32a}$$

$$C_{B2} = Ra_C \left\{ \left[ \frac{Q_{Cr} [1 + (2\phi_r - 1)\delta^2] - \delta^2}{1 + (\phi_r - 1)\delta} \right] (z - 1) + Q_{Cr} (1 - z^2) \right\}. \tag{32b}$$

The solution to the differential thermal equation system in the general case is too complicated to present here. This system has been studied by [Nield and Kuznetsov \(2014\)](#), who showed that weak LTNE did not change the basic solution significantly from the LTE solution,

$$T_{fB1} = Ra \left\{ \left[ \frac{Q_{fr} [1 + (2k_{fr} - 1)\delta^2] - k_{fr} \delta^2}{1 + (k_{fr} - 1)\delta} + 2\delta(1 - Q_{fr}) \right] z - z^2 \right\}, \tag{33a}$$

$$T_{sB1} = Ra \left\{ \left[ \frac{Q_{sr} [1 + (2k_{sr} - 1)\delta^2] - k_{sr} \delta^2}{1 + (k_{sr} - 1)\delta} + 2\delta(1 - Q_{sr}) \right] z - z^2 \right\}, \tag{33b}$$

$$T_{fB2} = Ra \left\{ \left[ \frac{Q_{fr} [1 + (2k_{fr} - 1)\delta^2] - k_{fr} \delta^2}{k_{fr} [1 + (k_{fr} - 1)\delta]} \right] (z - 1) + \frac{Q_{fr}}{k_{fr}} (1 - z^2) \right\}, \tag{33c}$$

$$T_{sB2} = Ra \left\{ \left[ \frac{Q_{sr} [1 + (2k_{sr} - 1)\delta^2] - k_{sr} \delta^2}{k_{sr} [1 + (k_{sr} - 1)\delta]} \right] (z - 1) + \frac{Q_{sr}}{k_{sr}} (1 - z^2) \right\}. \tag{33d}$$

Of particular interest for the stability problem is the distribution of the negative basic temperature gradient in the fluid phase, which we denote by  $F(z)$  and which is given by the linear expression  $Ra(2z - 1)$  in a homogeneous medium with uniform heating. From Eqs. (33a,c) we have

$$F_1(z) \equiv Ra f_1(z) = Ra \left\{ 2z - \frac{Q_{fr} [1 + (2k_{fr} - 1)\delta^2] - k_{fr} \delta^2}{1 + (k_{fr} - 1)\delta} - 2\delta(1 - Q_{fr}) \right\}, \tag{34a}$$

$$F_2(z) \equiv Ra f_2(z) = Ra \left\{ \frac{2Q_{fr}}{k_{fr}} z - \frac{Q_{fr} [1 + (2k_{fr} - 1)\delta^2] - k_{fr} \delta^2}{k_{fr} [1 + (k_{fr} - 1)\delta]} \right\}. \tag{34b}$$



Likewise the negative basic solutal gradient is  $G(z)$  where

$$G_1(z) \equiv Ra_C g_1(z) = Ra_C \left\{ 2z - \frac{\phi_r Q_{Cr} [1 + (2\phi_r - 1)\delta^2] - \phi_r \delta^2}{1 + (\phi_r - 1)\delta} - 2\delta(1 - \phi_r Q_{Cr}) \right\}, \tag{35a}$$

$$G_2(z) \equiv Ra_C g_2(z) = Ra_C \left\{ 2Q_{Cr} z - \frac{Q_{Cr} [1 + (2\phi_r - 1)\delta^2] - \delta^2}{1 + (\phi_r - 1)\delta} \right\}. \tag{35b}$$

### 2.3 Perturbation Equations

We now superimpose perturbations on the basic solution. We write

$$\mathbf{u} = \mathbf{u}', p = p_B + p', T_f = T_{fB} + T'_f, T_s = T_{sB} + T'_s, C = C_B + C', \tag{36}$$

substitute in Eqs. (13–17), and linearize by neglecting products of primed quantities. The following equations are obtained:

$$\nabla \cdot \mathbf{u}' = 0, \tag{37}$$

$$0 = -\nabla p' - \frac{1}{K} \mathbf{u}' + (T'_f + C') \hat{\mathbf{e}}_z, \tag{38}$$

$$\frac{\partial T'_f}{\partial t} + \frac{dT_{fB}}{dz} w' = \hat{k}_f \nabla^2 T'_f + \frac{\hat{h}}{\phi} N(T'_s - T'_f), \tag{39}$$

$$\hat{\epsilon} \alpha \frac{\partial T'_s}{\partial t} = \hat{k}_s \nabla^2 T'_s + \hat{\delta} \hat{h} \gamma N(T'_f - T'_s), \tag{40}$$

$$Le \frac{\partial C'}{\partial t} + \frac{Le}{\phi} \frac{dC_B}{dz} w' = \nabla^2 C', \tag{41}$$

$$w' = 0, T'_f = 0, T'_s = 0, C' = 0 \text{ at } z = 0 \text{ and at } z = 1. \tag{42}$$

The reader will note that, since there is no convection in the solid phase, the basic temperature gradient in the solid phase is not involved in the instability problem.

The seven unknowns  $u', v', w', p', T'_f, T'_s, C'$  can be reduced to four by operating on Eq. (38) with  $\hat{\mathbf{e}}_z \cdot \text{curl curl}$  and using the operator identity  $\text{curl curl} \equiv \text{grad div} - \nabla^2$  and Eq. (37). The result is

$$\nabla^2 w' = \hat{K} \nabla_H^2 (T'_f + C'). \tag{43}$$

Here  $\nabla_H^2$  is the two-dimensional Laplacian operator on the horizontal plane.

The boundary and interface conditions are

$$w'_1 = 0, T'_{f1} = 0, T'_{s1} = 0, C'_1 = 0 \text{ at } z = 0, \tag{44a,b,c,d}$$

$$w'_2 = 0, T'_{f2} = 0, T'_{s2} = 0, C'_2 = 0 \text{ at } z = 1, \tag{45a,b,c,d}$$

$$W'_1 = W'_2, \frac{\partial W'_1}{\partial z} = \frac{1}{K_r} \frac{\partial W'_2}{\partial z}, T'_{f1} = T'_{f2}, T'_{s1} = T'_{s2}, C'_1 = C'_2,$$

$$\frac{\partial T'_{f1}}{\partial z} = k_{fr} \frac{\partial T'_{f2}}{\partial z}, \frac{\partial T'_{s1}}{\partial z} = k_{sr} \frac{\partial T'_{s2}}{\partial z}, \frac{\partial C'_1}{\partial z} = \phi_r \frac{\partial C'_2}{\partial z} \text{ at } z = \delta.$$

$$\tag{46a,b,c,d,e,f,g,h}$$

The differential equations (43), (39–41) and the boundary and interface conditions (44–46) constitute a linear boundary-value problem that can be solved using the method of normal modes. We write

$$(w', T'_f, T'_s, C') = [W(z), \Theta_f(z), \Theta_s(z), \Gamma(z)] \exp(st + ilx + imy), \tag{47}$$

and substitute into the differential equations to obtain

$$(D^2 - a^2)W + \hat{K}a^2\Theta_f + \hat{K}a^2\Gamma = 0, \tag{48}$$

$$-\frac{dT_{fB}}{dz}W + \left( \hat{k}_f(D^2 - a^2) - s - \frac{\hat{h}}{\hat{\phi}}N \right)\Theta_f + \frac{\hat{h}}{\hat{\phi}}N\Theta_s = 0, \tag{49}$$

$$\hat{\delta}\hat{h}\gamma N\Theta_f + \left[ \hat{k}_s(D^2 - a^2) - \hat{\epsilon}\alpha s - \hat{\delta}\hat{h}\gamma N \right]\Theta_s = 0, \tag{50}$$

$$-\frac{dC_B}{dz}W + \left[ \frac{\hat{\phi}}{Le}(D^2 - a^2) - \hat{\phi}s \right]\Gamma = 0, \tag{51}$$

where

$$D \equiv \frac{d}{dz} \text{ and } a = (l^2 + m^2)^{1/2}. \tag{52}$$

Thus  $a$  is a dimensionless horizontal wavenumber.

The boundary and interface conditions are

$$W_1 = 0, \Theta_{f1} = 0, \Theta_{s1} = 0, \Gamma_1 = 0 \text{ at } z = 0, \tag{53a,b,c,d}$$

$$W_2 = 0, \Theta_{f2} = 0, \Theta_{s2} = 0, \Gamma_2 = 0 \text{ at } z = 1, \tag{54a,b,c,d}$$

$$W_1 = W_2, (1/K_1)DW_1 = (1/K_2)DW_2, \Theta_{f1} = \Theta_{f2}, \Theta_{s1} = \Theta_{s2}, \Gamma_1 = \Gamma_2,$$

$$k_{f1}D\Theta_{f1} = k_{f2}D\Theta_{f2}, k_{s1}D\Theta_{s1} = k_{s2}D\Theta_{s2}, \phi_1D\Gamma_1 = \phi_2D\Gamma_2 \text{ at } z = \delta.$$

$$\tag{55a,b,c,d,e,f,g,h}$$

For neutral stability the real part of  $s$  is zero. Hence we write  $s = i\omega$ , where  $\omega$  is real and is a dimensionless frequency. Our main objective is to investigate the relative importance of the various heterogeneity effects, and we would expect that these effects would be maximized for the case when the thermal and solutal buoyancy forces aid (rather than oppose) each other, that is for the non-oscillatory case. For this reason, and also because of the large number of parameters that are involved, we confine our attention to the case of non-oscillatory instability. The oscillatory case can be left for future investigation.

Accordingly, we put  $\omega = 0$ . As a result of this, the parameters  $\hat{\epsilon}$  and  $\alpha$  that appear in Eq. (50) now drop out of the system of differential equations.

We employed a Galerkin-type weighted residuals method to obtain an approximate solution to the system of Eqs. (48–51), (53–55). This method has been employed extensively in our previous papers (e.g. Kuznetsov and Nield 2013, 2014, 2015; Nield and Kuznetsov 2014, 2015), and so for brevity the details are omitted here. The idea is to choose trial functions that satisfy the boundary and interface conditions exactly (in our case low-order polynomials) and solve the differential equations exactly in an averaged sense, by imposing the condition that the residuals are orthogonal to the trial functions. The result is a set of homogeneous equations whose non-trivial solution leads to an eigenvalue equation with Ra as the eigenvalue. Thus Ra is found in terms of the other parameters.

### 3 Results and Discussion

Because of the large parameter space, we simplified the analysis. In order to have a tractable analysis, we employed a second-order Galerkin approximation. We believe that this relatively severe approximation is acceptable in this work because we are concerned just with sorting

out the major effects of heterogeneity and LTNE, and hence it is relative changes to, rather than absolute values of, the critical Rayleigh number that are of interest. The eigenvalue equation then takes the form of the vanishing of a determinant of order 8. We solved this numerically to obtain values of Ra.

We recover the homogeneous results when we set the heterogeneity ratios [those quantities defined in Eq. (19)] equal to unity and take one of the limits, either  $\delta$  tends to zero or  $\delta$  tends to 1,  $N$  tends to zero, or both  $N$  and  $\gamma$  tend to infinity. Also, for our investigation of the interaction between LTNE and heterogeneity, we may take as typical values  $\delta = 0.5, N = 1, \gamma = 1$ . We also fix  $Le = 1$ . This value is taken for illustrative purposes. In practical cases the value of Le will be greater than unity.

We now confine our attention to some special cases.

### 3.1 Homogeneity and Local Thermal Equilibrium

In this case we have

$$T_B = Ra(z - z^2), C_B = Ra_C(z - z^2). \tag{56}$$

We write

$$\tilde{\Theta} = \frac{\Theta}{Ra}, \tilde{\Gamma} = \frac{Le\Gamma}{Ra_C}. \tag{57}$$

Then Eqs. (48–51) become

$$(D^2 - a^2) W + a^2 \left( Ra\tilde{\Theta} + \frac{Ra_C}{Le}\tilde{\Gamma} \right) = 0, \tag{58}$$

$$(2z - 1) W + (D^2 - a^2) \tilde{\Theta} = 0, \tag{59}$$

$$(2z - 1) W + \frac{1}{Le} (D^2 - a^2) \tilde{\Gamma} = 0. \tag{60}$$

Eliminating  $\tilde{\Theta}$  and  $\tilde{\Gamma}$  between these equations we get

$$(D^2 - a^2)^2 W + a^2 (Ra + Ra_C) (1 - 2z) W = 0. \tag{61}$$

Using Eq. (58) we see that the boundary conditions on  $W$  are now

$$W = 0, D^2 W = 0 \text{ at } z = 0 \text{ and at } z = 1. \tag{62}$$

We observe that we have the same differential equation system as for the single-diffusive problem, but now the thermal Rayleigh number Ra is replaced by an effective combined Rayleigh number  $Ra_{eff}$  defined by

$$Ra_{eff} = Ra + Ra_C. \tag{63}$$

The critical Rayleigh number for the thermal problem was found by [Kulacki and Ramchandani \(1975\)](#) to be 235.67, obtained at a critical wavenumber 4.67. Thus for the double-diffusive case, the critical combined Rayleigh number is 235.67. In other words, the non-oscillatory stability boundary is

$$Ra + Ra_C = 235.67. \tag{64}$$

In the same way, one can readily show that the oscillatory instability boundary is given by

$$\frac{Le}{Le + 1} Ra + \frac{1}{Le + 1} Ra_C = 235.67 \tag{65}$$

provided that

$$Ra + Ra_C < 235.67. \quad (66)$$

These results mirror those for the bottom-heated/top-soluted problem given by Eqs. (9.20) and (9.21) of [Nield and Bejan \(2013\)](#).

### 3.2 Weak Heterogeneity and Weak Local Thermal Non-equilibrium

For the case

$$\begin{aligned} k_{fr} &= 1 + \varepsilon_{fk}, k_{sr} = 1 + \varepsilon_{sk}, K_r = 1 + \varepsilon_K, Q_{fr} = 1 + \varepsilon_{fQ}, Q_{Cr} = 1 + \varepsilon_{CQ}, \\ h_r &= 1 + \varepsilon_h, \phi_r = 1 + \varepsilon_\phi, \delta_r = 1 + \varepsilon_\delta, \end{aligned} \quad (67)$$

where  $\varepsilon_{fk}$ ,  $\varepsilon_{sk}$ ,  $\varepsilon_K$ ,  $\varepsilon_{fQ}$ ,  $\varepsilon_{CQ}$ ,  $\varepsilon_h$ ,  $\varepsilon_\phi$ ,  $\varepsilon_\delta$ , are all small compared with unity and with  $a$  fixed at the value 4.67, we obtained the following approximate expressions for the critical combined Rayleigh number.

For  $Ra_C = 0$ ,  $\delta = 0.1$ ,

$$\begin{aligned} Ra + Ra_C &= 251.9 + 422.0\varepsilon_{fk} + 0.1\varepsilon_{sk} - 252.4\varepsilon_K - 243.6\varepsilon_{fQ} \\ &\quad + 5.5\varepsilon_h - 5.6\varepsilon_\phi - 0.1\varepsilon_\delta. \end{aligned} \quad (68a)$$

For  $Ra_C = 0$ ,  $\delta = 0.5$ ,

$$\begin{aligned} Ra + Ra_C &= 251.9 + 275.1\varepsilon_{fk} + 0.1\varepsilon_{sk} - 213.5\varepsilon_K - 67.7\varepsilon_{fQ} \\ &\quad + 5.0\varepsilon_h - 5.1\varepsilon_\phi - 0.1\varepsilon_\delta. \end{aligned} \quad (68b)$$

For  $Ra_C = 0$ ,  $\delta = 0.9$ ,

$$\begin{aligned} Ra + Ra_C &= 251.9 + 18.5\varepsilon_{fk} + 0.0\varepsilon_{sk} - 62.5\varepsilon_K + 6.9\varepsilon_{fQ} \\ &\quad + 0.2\varepsilon_h - 0.2\varepsilon_\phi - 0.0\varepsilon_\delta. \end{aligned} \quad (68c)$$

These results are consistent with those obtained by [Kuznetsov and Nield \(2014\)](#) for the single-diffusive problem.

We also obtained the following results:

For  $Ra_C = 100$ ,  $\delta = 0.1$ ,

$$\begin{aligned} Ra + Ra_C &= 249.6 + 250.0\varepsilon_{fk} + 0.1\varepsilon_{sk} - 252.4\varepsilon_K - 144.7\varepsilon_{fQ} \\ &\quad + 3.3\varepsilon_h + 71.3\varepsilon_\phi - 0.1\varepsilon_\delta - 98.9\varepsilon_{CQ}. \end{aligned} \quad (69a)$$

For  $Ra_C = 100$ ,  $\delta = 0.5$ ,

$$\begin{aligned} Ra + Ra_C &= 249.6 + 163.4\varepsilon_{fk} + 0.1\varepsilon_{sk} - 213.6\varepsilon_K - 40.2\varepsilon_{fQ} \\ &\quad + 3.0\varepsilon_h + 83.0\varepsilon_\phi - 0.1\varepsilon_\delta - 27.3\varepsilon_{CQ}. \end{aligned} \quad (69b)$$

For  $Ra_C = 100$ ,  $\delta = 0.9$ ,

$$\begin{aligned} Ra + Ra_C &= 249.6 + 11.0\varepsilon_{fk} + 0.0\varepsilon_{sk} - 62.5\varepsilon_K + 4.1\varepsilon_{fQ} \\ &\quad + 0.1\varepsilon_h + 10.5\varepsilon_\phi - 0.0\varepsilon_\delta + 2.8\varepsilon_{CQ}. \end{aligned} \quad (69c)$$

We see immediately that weak heterogeneity of the interphase heat transfer coefficient  $h$ , the solid thermal conductivity  $k_s$  and the volume fraction  $\delta$  each have little effect on stability. Accordingly we can now concentrate on the heterogeneity of the remaining quantities, namely

**Table 1** Critical values of the combined Rayleigh number for  $\delta = 0.5$ ,  $N = 10$ ,  $\gamma = 10$ ,  $K_r = 1$ ,  $k_{fr} = 1$ ,  $k_{sr} = 1$ ,  $h_r = 1$ ,  $\delta_r = 1$ ,  $Le = 1$ ,  $Ra_C = 100$ : comparison between the analytical and the numerical solution

$Q_{fr}$	$Q_{Cr}$	$\phi_r$	$Ra + Ra_C$ analytical	$Ra + Ra_C$ numerical	% Error
1.1	1.1	1.1	251.15	229.24	9.6
1.1	1.1	0.9	234.55	227.71	3.0
1.1	0.9	1.1	256.61	243.44	5.4
1.1	0.9	0.9	240.01	241.30	0.5
0.9	1.1	1.1	259.19	248.48	4.3
0.9	1.1	0.9	242.59	246.74	1.7
0.9	0.9	1.1	264.65	264.48	0.0
0.9	0.9	0.9	248.05	262.02	5.3

the fluid thermal conductivity, the permeability, the source strength in the fluid phase, the porosity and the concentration source strength.

Comparison of Eqs. (69a–c) with (68a–c) shows that the constant and the permeability coefficient are little altered, as one would expect. When the solutal Rayleigh number is increased, the fluid conductivity and the fluid-phase heat-source-strength coefficients are reduced in magnitude and the porosity coefficient is increased. Also, of course, the heterogeneity of concentration source strength becomes effective.

Further, from the signs of the coefficients in Eqs. (68a–c) and (69a–c), we make the following conclusions. An increase in permeability in the upwards direction is destabilizing, while an increase in fluid thermal conductivity in the upwards direction is stabilizing. An increase in the upward direction of the heat source strength in the fluid phase is generally destabilizing. These trends, noted by [Kuznetsov and Nield \(2014\)](#), are in agreement with our expectation. With internal heating, the basic temperature gradient is positive in the upper portion of the domain, and so anything that aids the onset of convection in the upper portion is expected to be destabilizing. We also see that an increase in the upward direction of the concentration source strength is generally destabilizing.

A validation of the correlations expressed by Eqs. (68a–c) and (69a–c) is provided by a comparison with the results obtained by using a fully numerical solution of Eqs. (48–55). Numerical results with a high accuracy have been obtained by means of a Runge–Kutta solver coupled with the shooting method. This numerical procedure has been performed by employing the software package Mathematica 10 (© Wolfram Research, Champaign, IL). More details on this method can be found in the literature as, for example, [Straughan \(2008\)](#), [Rees and Bassom \(2000\)](#) and [Barletta and Storesletten \(2011\)](#). Table 1 reveals that the discrepancy is smaller than 10%. Higher discrepancies are found when the heterogeneity parameters become higher. For this reason, the analysis for strong heterogeneity performed in the next section was carried out numerically by employing the highly accurate numerical solver. The initial guess for the shooting method was generated by the second-order weighted residuals solution described at the beginning of this section.

### 3.3 Strong Heterogeneity

We consider the case of layers of equal thickness ( $\delta = 0.5$ ), where the variation of each heterogeneity parameter is doubled or halved, and with the LTNE values set at  $N = 1$ ,  $\gamma = 1$  and with  $Le = 1$ . Since our weak heterogeneity results have shown that variation in  $k_s$ ,  $h$  or  $\delta$

**Table 2** Critical values of the combined Rayleigh number and the corresponding wavenumber for various ratios of the heat source strength in the fluid phase, concentration source strength and porosity. Case  $\delta = 0.5, N = 1, \gamma = 1, K_r = 1, k_{fr} = 1, k_{sr} = 1, h_r = 1, \delta_r = 1, Le=1, Ra_C = 100$

$Q_{fr}$	$Q_C$	$\phi_r$	Analytical (initial guess)		Numerical	
			$Ra + Ra_C$	$a_c$	$Ra + Ra_C$	$a_c$
0.5	0.5	0.5	194	4.38	334.8	5.17
0.5	0.5	1	283	4.26	351.5	5.28
0.5	0.5	2	331	4.22	366.2	5.35
0.5	1	0.5	185	4.58	298.5	4.92
0.5	1	1	271	4.39	306.4	5.05
0.5	1	2	321	4.31	313.5	5.17
0.5	2	0.5	159	4.92	208.6	4.32
0.5	2	1	241	4.62	202.5	4.52
0.5	2	2	297	4.45	198.4	4.76
1	0.5	0.5	184	4.50	261.1	4.83
1	0.5	1	263	4.47	273.0	4.90
1	0.5	2	305	4.47	283.6	4.93
1	1	0.5	174	4.67	232.7	4.62
1	1	1	250	4.57	238.7	4.72
1	1	2	294	4.52	244.5	4.82
1	2	0.5	150	4.97	166.6	4.15
1	2	1	221	4.73	164.2	4.34
1	2	2	270	4.61	163.1	4.58
2	0.5	0.5	167	4.65	195.8	4.55
2	0.5	1	228	4.70	202.6	4.56
2	0.5	2	260	4.74	208.5	4.55
2	1	0.5	158	4.79	177.3	4.38
2	1	1	216	4.76	180.8	4.45
2	1	2	250	4.76	184.4	4.51
2	2	0.5	138	5.03	136.7	4.03
2	2	1	193	4.86	135.8	4.21
2	2	2	230	4.79	135.9	4.44

is not important, we have set  $k_{sr} = 1, h_r = 1, \delta_r = 1$  for our subsequent calculations. Further, since the effects of heterogeneity of  $K$  and  $k_f$  are already well understood (see [Kuznetsov and Nield 2014](#)), we also set  $K_r = 1, k_{fr} = 1$ . This leaves us with the heterogeneity of  $Q_f, Q_C$  and  $\phi$  to be examined in more detail. We obtained the results presented in Table 2.

These results show that, in moving from region 1 to region 2, increase in  $\phi$  is stabilizing (increasing the critical Rayleigh number), while increase in any of  $Q_f$  or  $Q_C$  is destabilizing (decreasing the critical Rayleigh number). The effect of heterogeneity of  $\phi$  is substantial when double diffusion comes into play. These trends are in accord with those obtained for weak heterogeneity. The source effects are in accord with our expectation. A more intense heat or concentration source in the upper region (where the vertical basic temperature gradient is negative) aids the onset of convection. The effect of porosity heterogeneity is more subtle and the trend was not anticipated. It appears to be a consequence of the fact that the convective

**Fig. 1** Plots of the critical combined Rayleigh number  $Ra + Ra_C$  (a) and the critical wavenumber  $a_c$  (b) versus fluid heat source strength ratio  $Q_{fr}$  for various values of the porosity ratio  $\phi_r$ . Case  $\delta = 0.5, N = 1, \gamma = 1, K_r = 1, k_{fr} = 1, k_{sr} = 1, h_r = 1, \delta_r = 1, Le = 1, Q_{Cr} = 1, Ra_C = 100$

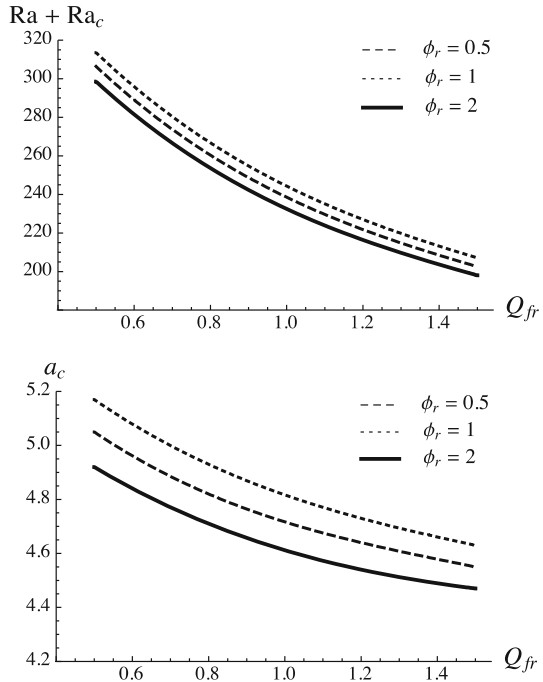
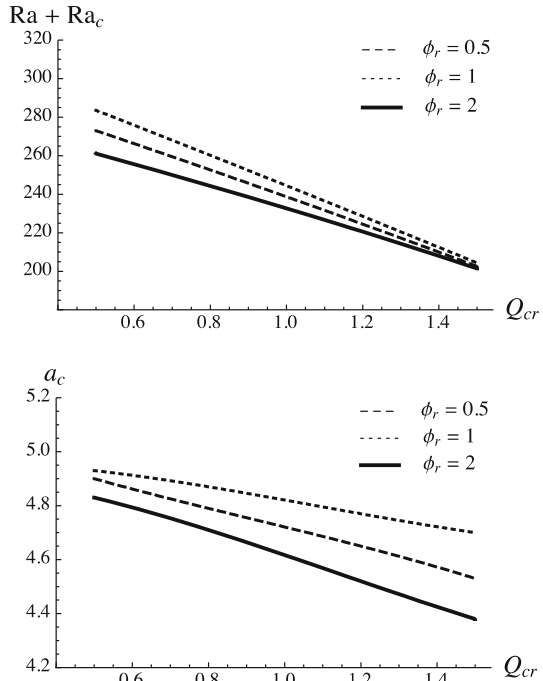


**Fig. 2** Plots of the critical combined Rayleigh number  $Ra + Ra_C$  (a) and the critical wavenumber  $a_c$  (b) versus concentration source strength ratio  $Q_{Cr}$  for various values of the porosity ratio  $\phi_r$ . Case  $\delta = 0.5, N = 1, \gamma = 1, K_r = 1, k_{fr} = 1, k_{sr} = 1, h_r = 1, \delta_r = 1, Le = 1, Q_{fr} = 1, Ra_C = 100$



transfer of solute concentration occurs only in the fluid phase. Thus the greater the porosity, the more the solutal buoyancy effect is weakened by being more spread out.

The critical wavenumber is affected to a lesser degree. Increase in either  $Q_f$  or  $Q_C$  results in an increase in that wavenumber, while increase in  $\phi$  leads to a variable change in the critical wavenumber.

In Figs. 1 and 2 we have plotted curves showing the variation of the critical combined Rayleigh number and the corresponding critical wavenumber with the most critical parameters. These show in more accessible format the trends shown in Table 2.

## 4 Conclusion

We have investigated the interaction between the effects of heterogeneity and local thermal non-equilibrium on the onset of double-diffusive convection in a porous medium consisting of two horizontal layers with volumetric heat and solute sources. There is a large parameters space, and in performing our investigations we found which parameters are important; this can be crucial for further numerical investigations of this system. We found that, as in the case of single-diffusive convection, major effects result from heterogeneity of permeability, fluid thermal conductivity and heat source strength in the fluid phases. With double diffusion there are additional major effects from the heterogeneity of solutal source strength and the heterogeneity of porosity (as distinct from heterogeneity of permeability). A lesser effect results from heterogeneity of the interphase heat transfer coefficient. Heterogeneity of solid thermal conductivity and heterogeneity of heat source strength in the solid phase are relatively unimportant. Our results also show in which direction the changes in the effective combined Rayleigh number will occur and the likely magnitude of those changes.

We remark that further complications would arise if one included the effect of throughflow.

**Acknowledgments** A.V.K. gratefully acknowledges the support of the Alexander von Humboldt Foundation through the Humboldt Research Award.

## References

- Barletta, A., Storesletten, L.: Thermoconvective instabilities in an inclined porous channel heated from below. *Int. J. Heat Mass Transf.* **54**, 2724–2733 (2011)
- Kulacki, F., Ramchandani, R.: Hydrodynamic instability in a porous layer saturated with a heat generating fluid. *Thermo Fluid Dyn.* **8**, 179–185 (1975)
- Kuznetsov, A.V., Nield, D.A.: The effect of strong heterogeneity on the onset of convection induced by internal heating in a porous medium: a layered model. *Transp. Porous Media* **99**, 85–100 (2013)
- Kuznetsov, A.V., Nield, D.A.: Local thermal non-equilibrium and heterogeneity effects on the onset of convection in an internally heated porous medium. *Transp. Porous Media* **102**, 15–30 (2014)
- Kuznetsov, A.V., Nield, D.A.: Local thermal non-equilibrium effects on the onset of convection in an internally heated layered porous medium with vertical throughflow. *Int. J. Therm. Sci.* **92**, 97–105 (2015)
- Nield, D.A.: Effects of local thermal nonequilibrium in steady convective processes in a saturated porous medium: forced convection in a channel. *J. Porous Media* **1**, 181–186 (1998)
- Nield, D.A.: A note on local thermal non-equilibrium in porous media near boundaries and interfaces. *Transp. Porous Media* **95**, 581–584 (2012)
- Nield, D.A., Bejan, A.: *Convection in Porous Media*, 4th edn. Springer, New York (2013)
- Nield, D.A., Kuznetsov, A.V.: The effect of heterogeneity on the onset of convection induced by internal heating in a porous medium: a layered model. *Transp. Porous Media* **100**, 83–99 (2013)
- Nield, D.A., Kuznetsov, A.V.: Local thermal non-equilibrium and heterogeneity effects on the onset of convection in a layered porous medium. *Transp. Porous Media* **102**, 1–13 (2014)



- Nield, D.A., Kuznetsov, A.V.: Local thermal non-equilibrium and heterogeneity effects on the onset of convection in a layered porous medium with vertical throughflow. *J. Porous Media* **18**, 125–136 (2015)
- Nield, D.A., Kuznetsov, A.V., Barletta, A., Celli, M.: The effects of double diffusion and local thermal non-equilibrium on the onset of convection in a layered porous medium: non-oscillatory instability. *Transp. Porous Media* **107**, 261–279 (2015)
- Patil, P.M., Rees, D.A.S.: Linear instability of a horizontal thermal boundary layer formed by vertical throughflow in a porous medium: the effect of local thermal nonequilibrium. *Transp. Porous Media* **99**, 207–227 (2013)
- Rees, D.A.S., Bassom, A.P.: The onset of Darcy-Bénard convection in an inclined layer heated from below. *Acta Mech.* **144**, 103–118 (2000)
- Straughan, B.: *Stability and Wave Motion in Porous Media*. Springer, New York (2008)
- Vadász, P.: Heat conduction in nanofluid suspensions. *ASME J. Heat Transf.* **128**, 465–477 (2006)